# KOH CONCENTRATION EFFECT ON THE CYCLE LIFE OF NICKEL–HYDROGEN CELLS IV. RESULTS OF FAILURE ANALYSES

H. S. LIM* and S. A. VERZWYVELT

*Hughes Aircraft Company, Bldg. 231, P.O. Box 2999, Torrance, CA 90509 (U.S.A.)*

## Summary

Potassium hydroxide concentration effects on the cycle life of a $Ni/H_2$ cell have been studied by carrying out a cycle life test on ten $Ni/H_2$ boiler plate cells which contain electrolytes of various KOH concentrations. Failure analyses of these cells were carried out after completion of the life test, which accumulated up to 40 000 cycles at an 80% depth of discharge over a period of 3.7 years. These failure analyses included studies on changes of electrical characteristics of test cells, and component analyses after disassembly of the cell. The component analyses included visual inspections, dimensional changes, capacity measurements of nickel electrodes, scanning electron microscopy, BET surface area measurements, and chemical analyses. Results have indicated that failure mode and change in the nickel electrode varied as the concentration was varied, especially when the concentration was changed from 31% or higher to 26% or lower.

## Introduction

Long cycle life has been demanded for a $Ni/H_2$ cell at deep depth of discharge cycles, used in space-craft applications, especially for a low earth orbit (LEO). We have reported earlier that the cycle life of $Ni/H_2$ cells was improved tremendously by using lower KOH concentrations in electrolyte than the conventional 31% KOH [1]. The cycle life has been improved as much as nine times by simply changing the concentration to 26% (by weight) from a conventional value of 31%. A cycle life test has been completed for ten $Ni/H_2$ cells containing electrolytes of various KOH concentrations ranging from 21 to 36%. In the present paper, we report failure analysis results of these cells which include studies on changes of cell performance and cell components after cell disassembly. We have also studied the electrochemical behavior of the cycled nickel electrodes. This result will be reported later.

*Author to whom correspondence should be addressed.

0378-7753/90/$3.50 

## Effects of KOH concentration on cycle life

A cycle life test was carried out in a 45 min LEO regime at 80% depth of discharge on ten $Ni/H_2$ boiler plate cells containing electrolytes of 21 - 36% KOH. The test period covered 3 years and 8 months and accumulated up to 39 573 life cycles. Details of the cycle regime have been reported earlier [1]. Life test results are summarized in Table 1. All cells of relatively short cycle life (BP3 - 6) failed by low end-of-discharge voltage (EODV), while all cells of long cycle life (BP1, 2, 9, and 10) failed the cycling test due to a "soft" short formation which was indicated by rapid self-discharge. Fully charged cells discharged completely in 30 - 35 h. The effect of the concentration on cycle life is shown in Figs. 1 and 2. The cycle life to 0.9 V of EODV peaked at 26% KOH, showing tremendous improvement (about nine times) over the conventional electrolyte of 31% KOH, but the life decreased sharply when the concentration was lowered further below 26%. If the voltage criteria for failure was lowered to 0.5 V, however, KOH concentrations as low as 21% also gave the extreme long life (Fig. 2). This rather drastic change in cycle life by a small change in the voltage criteria was due to the development of a large capacity having a low discharge voltage (about 0.8 V) plateau, which is often referred to as "the second plateau" [1c].

TABLE 1

Life test results of $Ni/H_2$ cells at 80% depth-of-discharge

| Cell no. | [KOH] (%) | No. cycle to 0.9 V | No. cycle to 0.5 V | Total no. cycles | Failure mode |
|---|---|---|---|---|---|
| BP1 | 21 | 5047 | > 38191 | 38191 | Soft short |
| BP2 | 26 | 39230 | > 39573 | 39573 | Soft short |
| BP3 | 26 | 4329 | 9241 | 9241 | Low EODV |
| BP4 | 31 | 2979 | 3275 | 3286 | Low EODV |
| BP5 | 31 | 3620 | 4230 | 4230 | Low EODV |
| BP6 | 36 | 1268 | 1845 | 1845 | Low EODV |
| BP7* | 21 | 1037 | 6508 | 9402 | Low EODV |
| BP8 | 26 | > 30549 | > 30549 | 30549 | Removed |
| BP9 | 26 | 23598 | > 24594 | 24594 | Soft short |
| BP10 | 23.5 | 4803 | 28495 | 28495 | Soft short |

*Cycled at 70% depth-of-discharge (DOD) from 1644 to 4644 cycles and after 6508 cycles.

## Change of cell characteristics after life test

A series of duplicate to triplicate capacity measurements was carried out before, and after, the cycle life test using various charge and discharge rates in order to evaluate the rate effects on cell capacity. The charge rate effect was studied by measuring cell capacity at $C/2$ discharge rate to 1.0 V

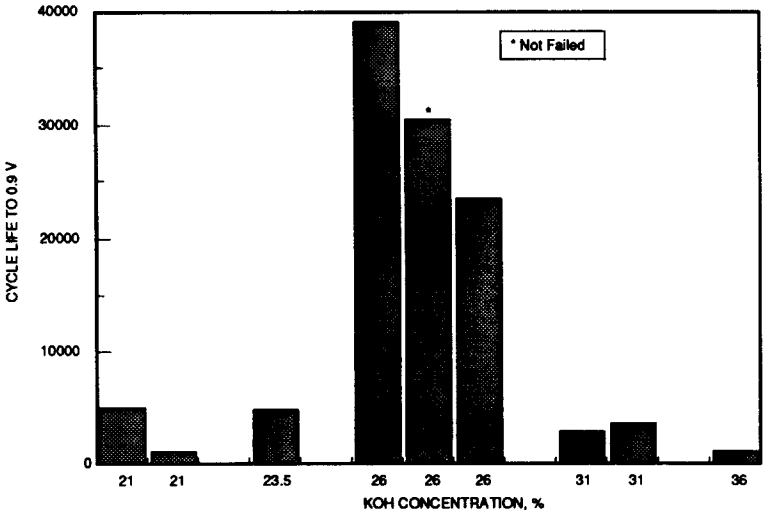


Fig. 1. Comparison of cycle life to 0.9 V of $Ni/H_2$ cells with various KOH concentrations in the electrolyte.

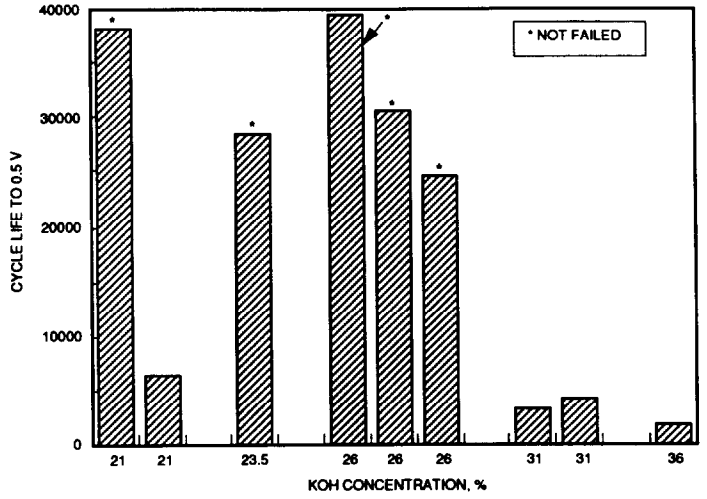


Fig. 2. Comparison of cycle life to 0.5 V of $Ni/H_2$ cells with various KOH concentrations in the electrolyte.

after charging at $C/10$ rate for 16 h, $C/2$ rate for 160 min, $C$ rate for 80 min, and 2 $C$ rate for 40 min. The discharge rate effect was studied by measuring cell capacity at various discharge rates ($C/10$, $C/2$, 1.0 $C$, 1.37 $C$, 2.0 $C$, 2.74 $C$, and 4.0 $C$) to 1.0 V after charging at the $C$ rate for 80 min. The internal resistance of the cells was evaluated from mid-discharge voltages at various discharge rates.

*Charge rate effects on cell capacity*

Initial and end-of-life (EOL) capacity values are plotted against charge rates in Figs. 3 and 4. The capacities of all cells improved as the charge rate increased from 0.1 to 0.5 *C* rate. This trend was more pronounced after the cycle test. Further increase in charge rate over 0.5 *C* did not affect the capacity of cells with high KOH concentrations (31 and 36%) while the capacity of cells with low KOH concentrations improved slightly at the 1 *C* rate. The capacities of all cells leveled off for charge rates between 1 and 2 *C*.

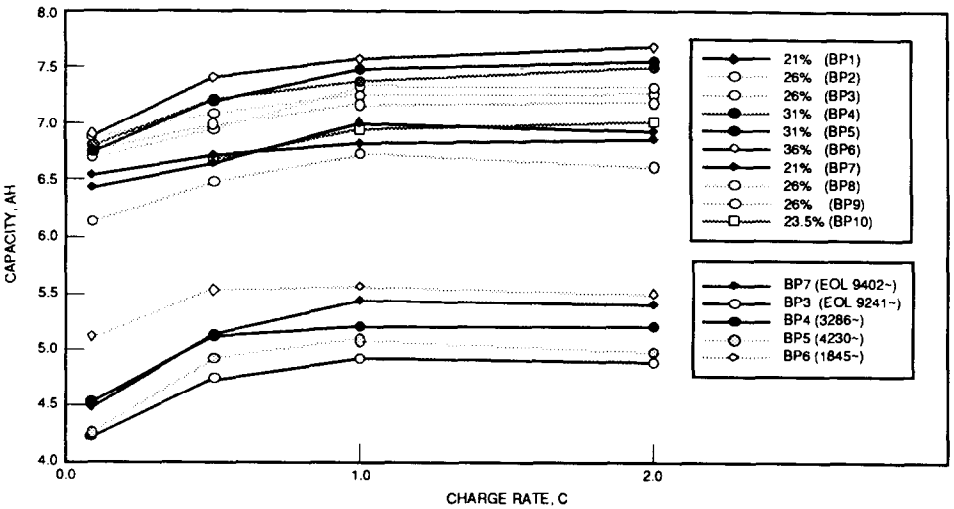


Fig. 3. Plots of initial and EOL capacities *vs.* charge rates. Capacity was measured by 0.5 *C* rate discharge to 1.0 V after charging at various rates: 0.1 *C* rate for 16 h, 0.5 *C* for 160 min, 1.0 *C* for 80 min, or 2.0 *C* for 40 min.

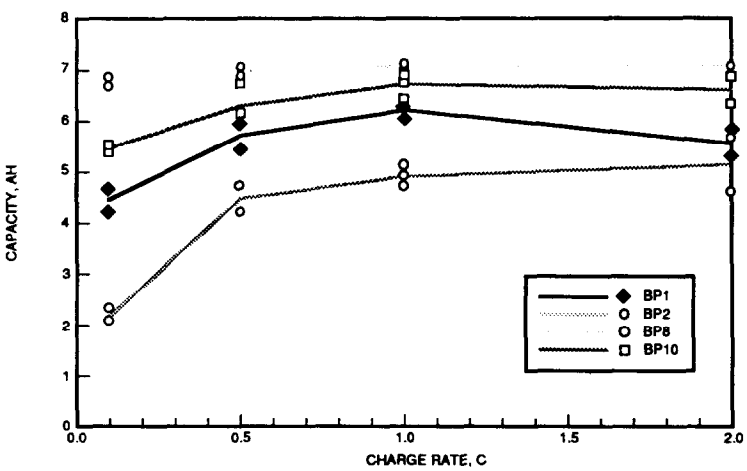


Fig. 4. Plots of EOL capacities *vs.* charge rates. Capacity was measured by 0.5 *C* rate discharge to 1.0 V after charging at various rates: 0.1 *C* rate for 16 h, 0.5 *C* for 160 min, 1.0 *C* for 80 min, or 2.0 *C* for 40 min.

Although absolute values of the capacity decreased after the life test, with the exception of BP 8 and 10, the general pattern of the charge rate dependence did not change with the cycle test.

*Effects of discharge rates on capacity*

Initial and EOL capacity values are plotted against discharge rates in Figs. 5 and 6. The capacity of cells in general decreased slightly as the discharge rate increased. This dependence of the capacity on discharge rate became more pronounced after the life test. We had also observed such dependence earlier with another group of 31% KOH cells [2].

*Cell resistance*

Plots of mid-discharge voltages (measured during the initial and EOL capacity tests) against the discharge current gave good straight lines as shown in Fig. 7, for example. The slopes of these lines represent the values of cell resistance. The cell resistances before and after the cycle life test are summarized in Table 2. Cell resistance did not appear to have changed significantly after the cycle life test except for BP1, BP3, and BP10. BP1 showed a significant reduction of the resistance. BP3, which had a defective current collector tab on one of the $H_2$ electrodes, showed a significant increase. Overall, the change in the cell resistance with cycling appeared to be too small to account either for the change of capacity dependence on discharge rate or to be the cause of cell failure.

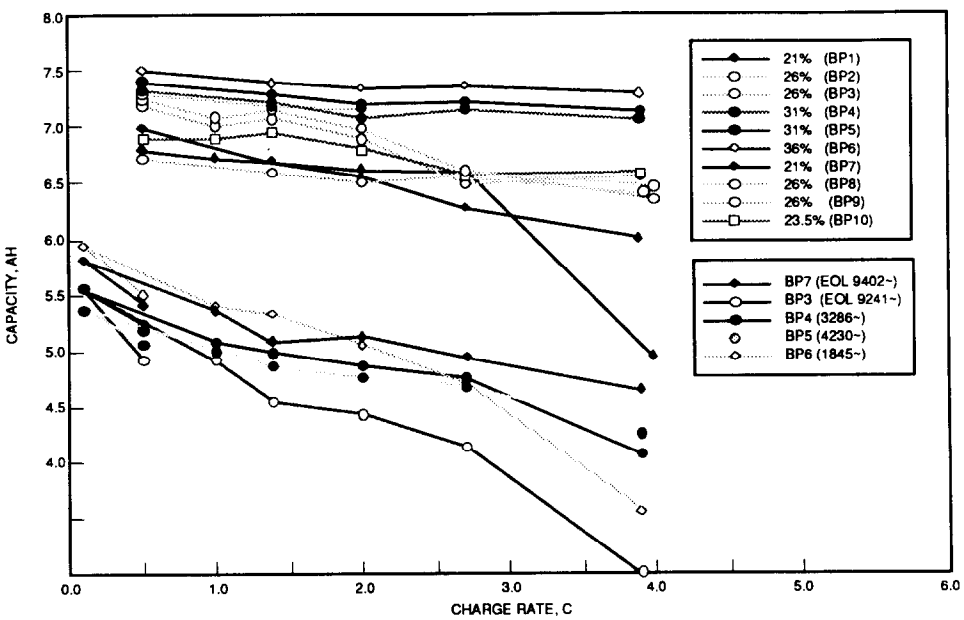


Fig. 5. Plots of initial and EOL capacities *vs.* charge rates. Capacity was measured by discharging cells at various rates to 1.0 V after 1.0 *C* rate charge for 80 min.

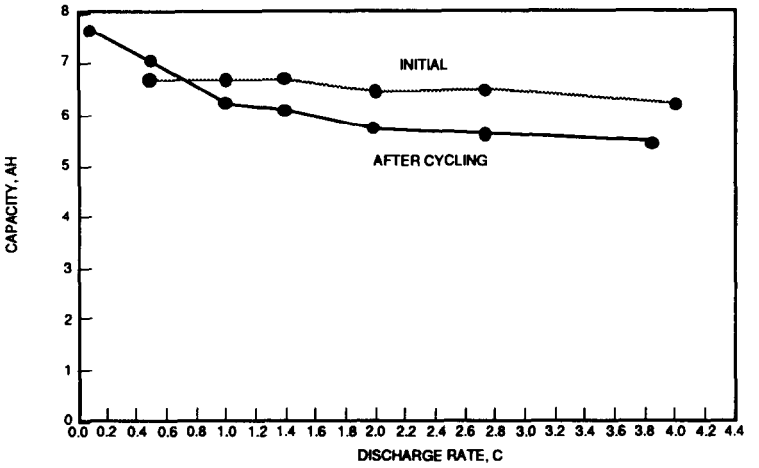


Fig. 6. Plots of initial and EOL capacities of BP8 *vs.* discharge rates. Capacity was measured by discharging the cell at various rates to 1.0 V after 1.0 *C* rate charge for 80 min.

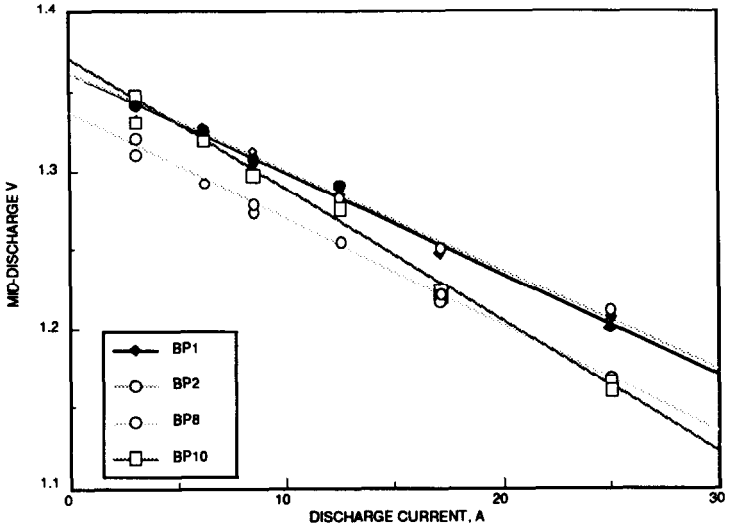


Fig. 7. Plots of mid-discharge voltages of test cells *vs.* discharge rates for end-of-life performance test.

## Component analyses after cell teardown

After the post-life-test capacity measurements, test cells were charged for 80 min at the *C* rate and then discharged at the *C*/2 rate to 0.5 V, followed by shorting them with a 1.0 Ω resistance for a minimum of 24 h before disassembly of the cells for component study. This study included visual inspections during the disassembly, electrode thickness measurements

TABLE 2

Cell resistance ($R$) measured from mid-discharge voltages

| Cell no. | KOH (%) | Number of cycles | Initial $R$ (mΩ) | EOL $R$ (mΩ) | Change (mΩ) | Cell P[a] (PSIG) |
|---|---|---|---|---|---|---|
| BP1 | 21.0 | 38191 | 10.83 | 6.36 | −4.47 | 615 |
| BP2 | 26.0 | 39573 | (5.89) | 6.26 | +0.37 | 705 |
| BP3 | 26.0 | 9241 | 7.53 | 9.69 | +2.16 | 130 |
| BP4 | 31.0 | 3286 | 7.15 | 8.26 | +1.11 | 150 |
| BP5 | 31.0 | 4230 | 7.09 | 6.96 | −0.13 | 225 |
| BP6 | 36.0 | 1845 | 7.61 | 8.49 | +0.88 | 160 |
| BP7 | 21.0 | 9402 | 7.30 | 7.14 | −0.16 | 130 |
| BP8 | 26.0 | 30549 | 6.59 | 6.71 | +0.12 | 0 |
| BP10 | 23.5 | 28495 | 6.57 | 8.24 | +1.67 | 635 |

[a]Pressure prior to disassembly.

(without washing and drying), scanning electron microscopy (SEM) of the cross-section of cell stacks, surface area measurements using the BET technique, measurements of nickel electrode capacity and discharge voltages in flooded electrolyte cells, and chemical analyses of the nickel electrodes.

*Visual inspections*

The conditions of the cell stack and its components have been inspected carefully during disassembly of cycled cells. These inspections included wetness of components, degree of loose, black, nickel active material ("black powder") on cell components, penetration of the active material through the separator, adhesion of the hydrogen electrode to the gas screen, and the integrity of nickel and hydrogen electrodes. Observations which appear to be important are summarized as follows:

- Wetness of the electrode and the degree of "black powder" formation increased noticeably as one approached the bottom of the stack (no. 6 unit cell) from the top (no. 1 unit cell). The observation on wetness change indicated that the gravitational effect on the electrolyte distribution is substantial, even in this relatively short stack. The observation on "black powder" formation appears to indicate that a wetter unit cell might have been used more heavily than a drier unit cell.
- Electrodes from BP7 (21% KOH; 9402 cycles) showed noticeably less "black powder" on the adjacent separator and in the gas screen than those from high KOH concentration cells which had a lower number of cycles. The black powder in the gas screen was found only in the peripheral area of the stack with BP7, but it was found all over the screen with the other cells which were cycled less than BP7. However, the 21% KOH cell (BP1; 38 191 cycles), which was cycled for much longer, showed heavy black powdering. It appears that the rate of black powder formation is reduced as the KOH concentration decreased.

• The electrical lead (tab) of #5 $H_2$ electrode of BP3 was not firmly attached (defective weld) to the electrode while its paired nickel electrode and separator appeared to be new (almost without the black powder). This observation strongly indicates that the cause of the poor performance of this cell from the beginning was due to this poor electrical contact. BP3 shoule be considered as an anomalous cell.

• All nickel electrodes from cells which had extremely long cycle lives ($\geqslant$24 594 cycles) showed a "mushy" appearance, indicating that some active material had loosened and squeezed out of the sinter structure. This indication was confirmed by scanning electron microscopic (SEM) pictures, as will be discussed later in this report.

• All cells which had extremely long cycle lives ($\geqslant$24 594 cycles) showed the following: the outer edges of the gas screen were welded to the Teflon layer of the $H_2$ electrodes; damage, with partially lost electrode material, was apparent on parts of the peripheral area of electrode stacks; the outer, coined nickel electrodes were badly eroded. These observations indicated that violent recombinations of $O_2$ with $H_2$ had occurred around the peripheral area of electrode stacks during the cycling test period.

*Pressure changes*

The gas pressure of test cells in the fully discharged state was measured, just before their disassembly, using a mechanical pressure gauge. This was done in order to determine the net pressure change during the cycle life test. The gas composition was analyzed using a gas chromatograph. Within experimental error the gas in all the cells was pure hydrogen. The results of pressure readings are shown in Table 2. Long cycled cells (BP1, 2, and 10) showed roughly 470 psi higher pressure than those of relatively short cycle life (BP4, 5, and 6). (BP8 might have leaked slowly.) Although the long term sealing reliability of presently used boiler plate cell cases was questionable, as discussed earlier [1b], the pressure increase in long cycled cells is real. This pressure increase appears to be due to nickel corrosion from the sintered plaques, probably according to eqn. (1):

$$Ni + 2H_2O \longrightarrow Ni(OH)_2 + H_2 \quad (1)$$

*Dimensional changes of stack components*

The thickness of nickel electrodes was measured by a micrometer at three different locations on each electrode before and after cycling. The thickness after cycling was measured both before and after rinsing out the electrolyte and drying. These two values agreed with each other within experimental error. The average values of these measurements for each electrode are given in Table 3. Long cycled electrodes (BP2 and BP8) showed expansion values up to 80% of the original thickness. These long cycled electrodes showed heavy extrusion of active material from the electrode into the gas screen voids. Typical gas screen imprints are clearly visible when the

TABLE 3

Nickel electrode expansion after cycle test in $Ni/H_2$ cells with various KOH concentrations

| Cell (% KOH) (cycle no.) | Electrode i.d. | Thickness after cycling[a] (mm) | Thickness before cycling (mm) | Expansion[a] (%) |
|---|---|---|---|---|
| BP1 (21%) | 28-05 (#1, top) | 1.166 | 0.761 | 53.4 |
| (31 191) | 28-04 (#2) | 1.141 | 0.758 | 50.5 |
| | 24-03 (#5) | 1.268 | 0.737 | 71.8 |
| | 24-01 (#6, bottom) | 1.225 | 0.751 | 63.2 |
| BP2 (26%) | 20-01 (#1) | 1.310 | 0.732 | 79.0 |
| (39 573) | 20-02 (#2) | 1.274 | 0.739 | 72.5 |
| | 19-05 (#5) | 1.341 | 0.737 | 81.8 |
| | 19-06 (#6) | 1.327 | 0.735 | 76.1 |
| BP3 (26%) | 25:01 (#1) | 0.930 | 0.768 | 21.1 |
| (9641) | 26-02 | 0.933 | 0.744 | 25.3 |
| | 35-03 (AN) | 0.762 | 0.750 | 1.6 |
| | 35-04 (#6) | 0.947 | 0.753 | 25.7 |
| BP4 (31%) | 25-09 (#1) | 0.837 | 0.727 | 15.1 |
| (3275) | 26-03 | 0.814 | 0.732 | 11.2 |
| | 26-09 | 0.819 | 0.755 | 8.5 |
| | 27-07 (#6) | 0.778 | 0.744 | 4.6 |
| BP5 (31%) | 22-02 (#1) | 0.809 | 0.738 | 9.6 |
| (4230) | 22-03 | 0.814 | 0.732 | 13.6 |
| | 22-09 | 0.785 | 0.721 | 8.9 |
| | 20-03 (#6) | 0.758 | 0.755 | 0.4 |
| BP6 (36%) | 27-03 (#1) | 0.816 | 0.744 | 9.6 |
| (1845) | 27-05 | 0.777 | 0.720 | 7.8 |
| | 35-08 | 0.785 | 0.724 | 8.4 |
| | 35-09 (#6) | 0.771 | 0.723 | 6.7 |
| BP7 (21%) | 05-05 (#1) | 0.876 | 0.748 | 17.2 |
| (9402) | 05-06 (#2) | 0.916 | 0.746 | 22.7 |
| | 21-07 (#3) | 0.929 | 0.755 | 23.1 |
| | 21-08 (#4) | 0.949 | 0.755 | 25.6 |
| BP8 (26%) | 21-05 (#1) | 1.225 | 0.728 | 68.2 |
| (30 549) | 21-01 (#2) | 1.286 | 0.762 | 68.7 |
| | 03-06 (#5) | 1.297 | 0.727 | 78.4 |
| | 03-02 (#6) | 1.304 | 0.719 | 81.3 |
| BP9 (26%) | 03-03 (#1) | 1.217 | 0.736 | 65.4 |
| (24 594) | 04-07 (#2) | 1.229 | 0.735 | 63.2 |
| | 04-07 (#5) | 1.233 | 0.741 | 66.4 |
| | 06-07 (#6) | 1.208 | 0.752 | 60.6 |
| BP10 (23.5%) | 04-03 (#1) | 1.330 | 0.751 | 77.2 |
| (28 495) | 16-05 (#2) | 1.281 | 0.736 | 74.1 |
| | 16-02 (#5) | 1.353 | 0.760 | 78.0 |
| | 16-09 (#6) | 1.285 | 0.746 | 72.1 |

[a]Measured values include extruded active material into voids of gas screen.

gas screen is separated from the electrode. The high expansion value (up to 80%) was due to the contribution of this extruded material.

Average electrode expansion values from individual cells are plotted against number of cycles in Fig. 8. The expansion values appear to fall on a straight line even though the individual cells have different KOH concentrations. This observation appears to indicate that the expansion rate on long term cycling is rather insensitive to KOH concentration, which is contrary to our earlier understanding [3 - 5]. Expansion itself does not appear to be the main cause of electrode or cell failure.

The thickness of the stack components, including the separator and gas screen, was also measured from an SEM micrograph of the cell stack cross-section. The results are shown in Fig. 9 as a function of the number of cycles. The unit cell dimension was generally unchanged with cycling. Nickel electrode expansion was again roughly linear with the number of cycles. The separator and gas screen were compressed as the nickel electrode expanded.

*Electrode capacity in a flooded cell*

The capacities of two nickel electrodes from each failed cell were measured in a flooded cell at $C/2$ discharge rate after charging at $C/10$ for 18 - 19 h. One electrode was from the top of the cell stack (#1) and the other was from the bottom of the stack (#6). Two to three capacities were measured in an electrolyte of the same KOH concentration as the original test cell and then all electrolytes were changed, using 31% KOH for the additional three capacities. The results are summarized in Table 4. With the exception of BP3, which was an anomalous cell, the capacity loss of nickel electrodes in low KOH concentration (21 - 26%) cells was relatively low and independent of the electrode position (#1 or #6) despite long cycling. With

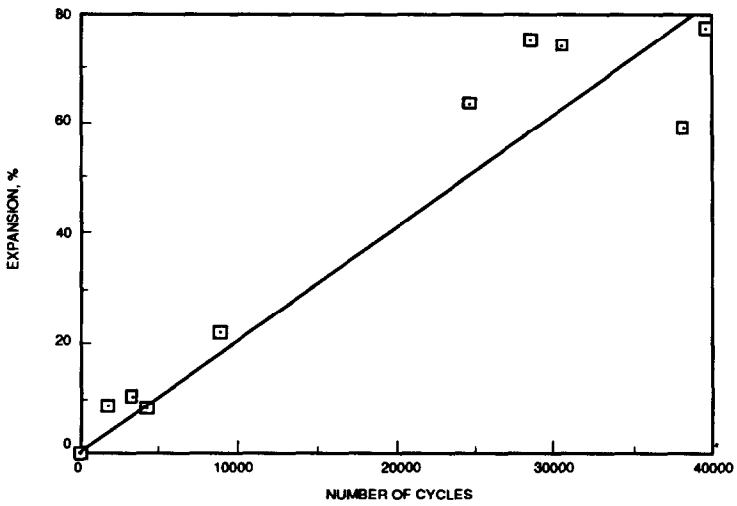


Fig. 8. A plot of nickel electrode expansion *vs.* number of cycles.

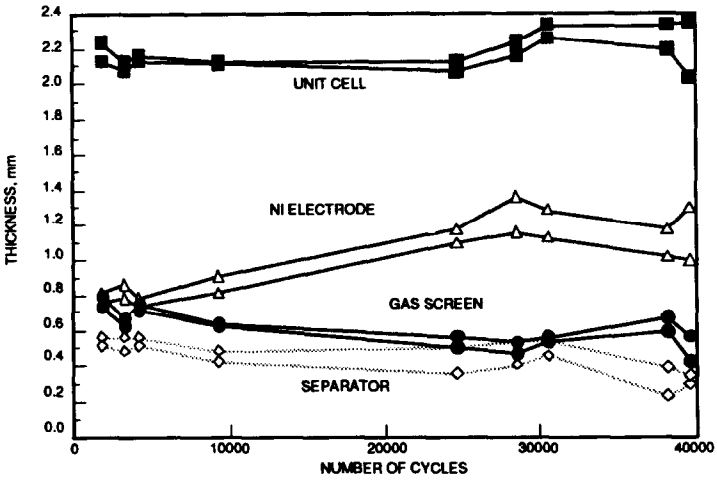


Fig. 9. Plots of the thickness of the cell stack components as a function of cycling.

TABLE 4

Flooded capacities of nickel electrodes from cycled cells
#1: Top electrode of the stack, #6 bottom electrode of the stack. A new electrode had an average value of 1.24 A h

| Cell no. (%) | KOH conc. (%) | Capacity of #1 electrode (A h) | | | | Capacity of #6 electrode (A h) | | | | Capacity ratio (#6/#1) |
|---|---|---|---|---|---|---|---|---|---|---|
| | | 1st | 2nd | 3rd | Av. | 1st | 2nd | 3rd | Av. | |
| BP1 | 21 | 1.17 | 1.18 | | 1.18 | 1.24 | 1.24 | | 1.24 | 1.05 |
| BP2 | 26 | 1.18 | 1.17 | | 1.17 | 1.25 | 1.24 | | 1.25 | 1.07 |
| BP3 | 26 | 0.99 | 1.00 | 1.00 | 1.00 | 0.70 | 0.69 | 0.70 | 0.70 | 0.70 |
| BP4 | 31 | 1.16 | 1.11 | 1.12 | 1.13 | 0.73 | 0.77 | 0.79 | 0.76 | 0.67 |
| BP5 | 31 | 0.98 | 0.96 | 0.98 | 0.97 | 0.69 | 0.70 | 0.71 | 0.70 | 0.72 |
| BP6 | 36 | 0.98 | 1.08 | 1.17 | 1.08 | 0.69 | 0.81 | 0.81 | 0.77 | 0.72 |
| BP7 | 21 | 0.95 | 0.93 | 0.93 | 0.94 | 1.01 | 1.02 | 1.01 | 1.01 | 1.08 |
| BP8 | 26 | 1.21 | 1.15 | | 1.18 | 1.13 | 1.11 | | 1.12 | 0.95 |
| BP10 | 23.5 | 1.26 | 1.26 | | 1.26 | 1.24 | 1.24 | | 1.24 | 0.98 |
| After changing electrolyte | | | | | | | | | | |
| BP1 | 31 | 1.11 | 1.10 | | 1.11 | 1.16 | 1.15 | | 1.16 | 1.04 |
| BP2 | 31 | 1.13 | 1.23 | | 1.18 | 1.16 | 1.15 | | 1.16 | 0.98 |
| BP3 | 31 | 1.02 | 1.04 | 1.03 | 1.03 | 0.75 | 0.77 | 0.77 | 0.76 | 0.74 |
| BP4 | 31 | 1.14 | 1.14 | 1.14 | 1.14 | 0.79 | 0.80 | 0.80 | 0.80 | 0.70 |
| BP5 | 31 | 1.01 | 1.03 | 1.03 | 1.02 | 0.72 | 0.72 | 0.72 | 0.72 | 0.72 |
| BP6 | 31 | 1.04 | 1.04 | 1.03 | 1.04 | 0.69 | 0.70 | 0.70 | 0.70 | 0.68 |
| BP7 | 31 | 1.02 | 1.06 | 1.05 | 1.04 | 1.03 | 1.09 | 1.08 | 1.07 | 1.03 |
| BP8 | 31 | 1.21 | 1.20 | | 1.21 | 1.06 | 1.05 | | 1.06 | 0.88 |
| BP10 | 31 | 1.21 | 1.20 | | 1.21 | 1.21 | 1.20 | | 1.21 | 1.00 |

higher KOH concentrations (31 - 36%), however, the capacity of the bottom (#6) nickel electrode was roughly 30% smaller than the top (#1) electrode of the same cell. It appears that the cause of this faster degradation of the electrodes from the bottom (#6) to the top (#1) of the stack resulted from the variation of the electrolyte content from the top to the bottom. Cell teardown showed that the bottom part (#6) of the stack had much more electrolyte than the top part (#1) due to gravitational segregation. The wetter electrode pair (#6) is expected to pass higher current throughout the cycle test than the drier pair (#1), which was in parallel electrical connection. This uneven current distribution would have caused heavier usage of the #6 electrode than #1. This heavy usage appears to cause a severe capacity decrease in higher KOH concentrations, while the decrease is relatively minor in low KOH concentrations. No apparent relationship was found between the capacity decrease and the electrode expansion.

*Chemical analyses*

The chemical composition of the electrolyte of the cycled cells is shown in Table 5. The overall electrolyte concentrations in long cycled cells (BP2, BP8, and BP10) were increased by 3 to 4% from the initial value, indicating possible nickel plaque corrosion. Carbonate concentration, which was negligible initially, increased slightly in all the cycled cells. The amount of carbonate build-up was roughly proportional to the logarithmic number of cycles, as shown in Fig. 10. A possible source of carbonate may result from plaque corrosion. Plaque may contain about 0.1 wt.% of carbon because it is made from carbonyl nickel powder (INCO Type 287) [6].

The results of chemical analyses of new and cycled nickel electrodes from test cells are shown in Table 6. Active material content (the amount of total ionic Ni and Co in the nickel electrode) is plotted against the number of cycles in Fig. 11. This content increased with cycling, indicating that nickel plaque may corrode gradually with cycling. Experimental data fit roughly to a linear corrosion rate of 0.1 Å/cycle (curve A of Fig. 11).

TABLE 5

Composition of electrolyte from cycled cells

| Cell no. | Initial conc. of KOH (%) | KOH as KOH (%) | $K_2CO_3$ as KOH (%) | Total $K^+$ ion as KOH (%) | Sampling technique |
|---|---|---|---|---|---|
| BP2 | 26 | 25.5 | 5.27 | 30.77 | Soxhlet[a] |
| BP3 | 26 | 23.6 | 2.7 | 26.3 | Bottom of cell |
| BP4 | 31 | 28.0 | 3.3 | 31.3 | Bottom of cell |
| BP6 | 36 | 33.2 | 2.5 | 35.7 | Bottom of cell |
| BP7 | 21 | 17.3 | 4.0 | 21.3 | Bottom of cell |
| BP8 | 26 | 24.03 | 5.07 | 29.1 | Soxhlet[a] |
| BP10 | 23.5 | 21.6 | 5.1 | 26.7 | Soxhlet[a] |

[a]Soxhlet extraction of #3 & 4 unit cells.

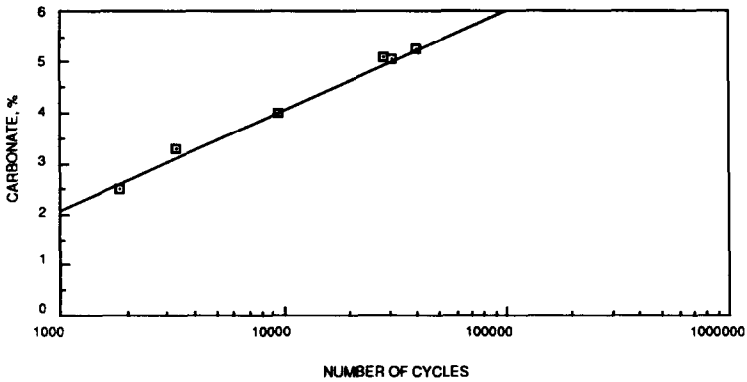


Fig. 10. A plot of carbonate build-up *vs.* number of cycles.

TABLE 6

Results of chemical analyses of new and cycled nickel electrodes from BP cells
Numerical values in this table indicate amounts in mmoles/g of active mass.

| | New 27-08 | BP1 | BP2 | PB4 | BP6 | BP8 | BP10 |
|---|---|---|---|---|---|---|---|
| Ni° (sinter) | | | | | | | |
| Titration (A) | 8.29 | 4.92 | 3.70 | 7.79 | 8.41 | 4.99 | 4.59 |
| AA | 8.20 | 4.59 | 3.27 | 6.49 | 7.47 | 4.59 | 4.20 |
| M (II & III); Titration (B) | 4.90 | 7.24 | 8.10 | 5.14 | 4.77 | 7.32 | 7.19 |
| Co (II & III); AA | 0.67 | 0.55 | 0.57 | 0.61 | 0.57 | 0.57 | 0.59 |
| M (III) | 1.50 | 0.90 | 1.78 | 0.58 | 0.80 | 2.60 | 1.40 |
| Total Ni & Co titration | 13.40 | 12.06 | 11.94 | 12.20 | 12.56 | 12.23 | 11.87 |
| (A) + (B) | 13.19 | 12.16 | 11.80 | 12.93 | 13.18 | 12.31 | 11.78 |
| (A)/[(A) + (B)] (%) | 62.85 | 40.46 | 31.36 | 60.25 | 63.81 | 40.54 | 38.96 |

Elemental analyses (spectrographic) were carried out on the outer edge of nickel electrodes from a few cycled BP cells in which soft shorts had developed to determine whether Pt was carried over to the nickel electrode from the adjacent $H_2$ electrode. The results from BP9 showed a considerable amount of Pt (0.25%); Pt was not detected from a new electrode, and was detected only in trace amounts (<0.01%) in electrodes from BP2 and BP5. Considering that both BP2 and BP9 had soft shorts, this non-uniform distribution of Pt might be due to violent $O_2$ recombination ("popping") at the peripheral edge and probably causing Pt migration.

*Scanning electron microscope (SEM)*

SEM pictures of a cross-section of cell stack components were taken as part of the failure analyses. Sample photographs of the components from

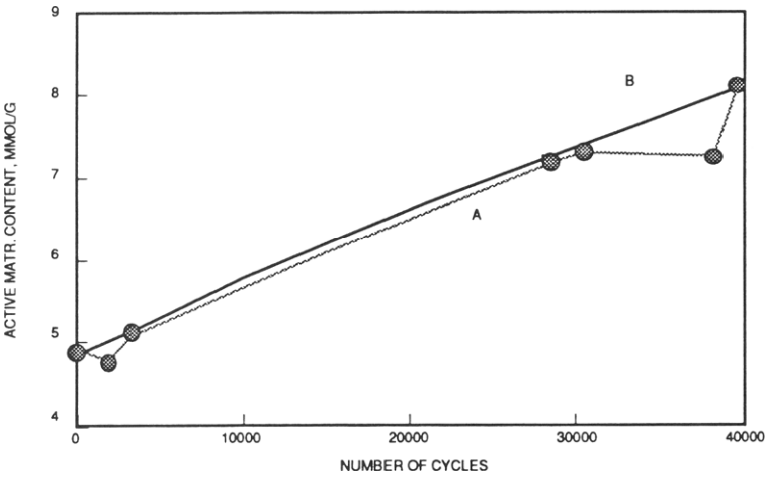


Fig. 11. A plot of active material content (total ionic nickel and cobalt) of nickel electrode *vs.* number of cycles.

cycled cells are shown in Figs. 12 - 14. BP6 (36%), which failed after relatively short cycling (1845 cycles), showed no apparent sign of expansion or deformation of stack components. However, long cycled cells, BP9 and BP2 (24 594 and 39 573 cycles, respectively) showed signs of heavy nickel electrode expansion, nickel active material migration, rupture of nickel sinter substrate, and deformation of other components such as the separator, the $H_2$ electrode, and gas screen material. It is interesting to note that despite the heavy expansion and sinter rupture in the long-cycled electrodes, they suffered only a relatively small capacity decrease, indicating that these changes do not directly cause electrode failure.

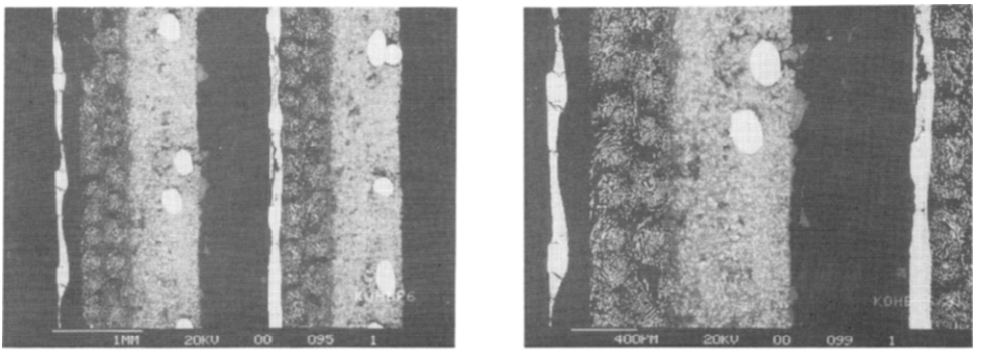


(a) (b)

Fig. 12. SEM cross-sectional view of (a) #3 and #4 cells and (b) expanded view of local area of BP6.

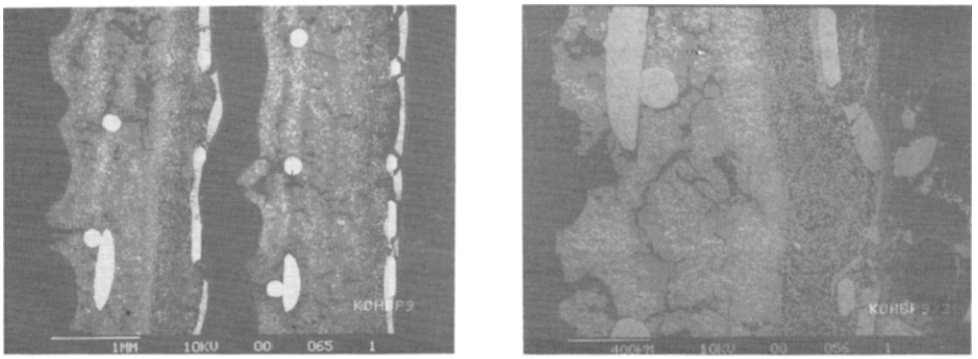

(a) (b)

Fig. 13. SEM cross-sectional view of (a) #3 and #4 cells and (b) expanded view of local area of BP9.

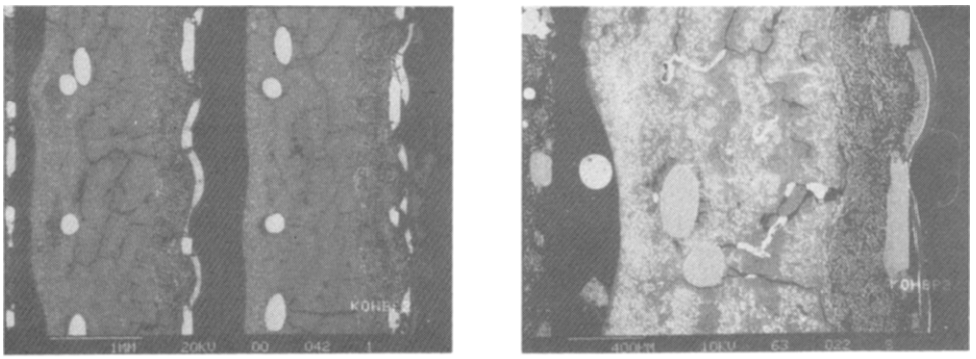

(a) (b)

Fig. 14. SEM cross-sectional view of (a) #3 and #4 cells and (b) expanded view of local area of BP2.

## Discussion

The cycle life of a nickel electrode increased greatly as the KOH concentration decreased in the electrolyte, although, as reported earlier, the initial capacity of a nickel electrode decreases slightly as the concentration decreases [1b]. The cycle life increased more than twice when the concentration was decreased from 36 to 31%. Although results with very low KOH concentration (21 - 23.5%) were complicated due to unusable low voltage secondary plateau formation [1c], the cycle life improved roughly nine times when the concentration was reduced to 26% from the conventional value of 31%.

The failure mechanisms of a $Ni/H_2$ cell with a low KOH concentration (26% or lower) and one with a high KOH concentration (31% or higher), appear to differ. High concentration KOH cells failed on cycling by a gradual fall of nickel electrode capacity after a relatively small number of cycles

(1845 - 4230), while low concentration cells failed on cycling, after a large number of cycles (mostly 25 000 - 40 000), by a "soft" short formation without an excessive capacity decrease of the nickel electrodes. Resulting from the large difference in the number of cycles, heavy electrode expansion, and active material migration and extrusion were observed in the long life, low-KOH concentration cells, but relatively small physical changes occurred in the failed nickel electrodes in the high KOH concentration cells. Much less "black powder" formation was observed in BP7 (21% KOH) after 9402 cycles than in BP4 (31% KOH), BP5 (31% KOH), and BP6 (36% KOH) which were tested for less than half the number of cycles, indicating that some physical changes occur at a much reduced rate in low KOH concentrations.

The observation that no significant cell internal resistance change occurs, despite heavy electrode expansion causing sinter rupture, and active material migration and extrusion, appears to indicate that the conductivity of nickel sinter may not be the controlling factor in electrode failure. We speculate that the capacity fading mechanism might involve crystallographic and micro-morphological changes in the active material. All long-life cells failed eventually on cycling due to a "soft" short formation without an excessive capacity decrease of the nickel electrodes, as shown in Table 4. The positive identification of Pt on a nickel electrode (spectrographic analysis) appears to indicate that the short might be due to Pt on the nickel electrode. The Pt might act as a hydrogen electrode while it is electrically shorted to the nickel electrode through a layer of high resistance nickel oxide/hydroxide material. An alternative mechanism might involve a short between nickel and hydrogen electrodes via extruded nickel active-material in the gas screen area.

## Acknowledgement

The authors acknowledge NASA-Lewis Research Center for its support for this study (Contract NAS 3-22238; Project Manager: John Smithrick).

## References

1 (a) H. S. Lim and S. A. Verzwyvelt, KOH concentration effect on the cycle life of nickel–hydrogen cells, *Proc. 20th IECEC, August, 1985*, p. 1.165; (b) H. S. Lim and S. A. Verzwyvelt, Cycle life of nickel–hydrogen cells. II. Accelerated cycle life test, *Proc. 21st IECEC, August, 1986*, p. 1601; (c) H. S. Lim and S. A. Verzwyvelt, *J. Power Sources, 22* (1988) 213.

2 (a) H. S. Lim, Long life nickel electrodes for nickel–hydrogen cells, *Final Rep. of Phase I, NAS 3-22238, NASA Cr-174815. December, 1984*; (b) H. S. Lim and S. A. Verzwyvelt, Long life nickel electrodes for a nickel–hydrogen cell: I. Initial Performance, *Proc. 18th IECEC, August, 1983*, p. 1543; (c) H. S. Lim and

S. A. Verzwyvelt, Long life nickel electrodes for a nickel–hydrogen cell: cycle life test, *Proc. 31st Power Sources Symp., Cherry Hill, NJ, June, 1984*, p. 157; (d) H. S. Lim and S. A. Verzwyvelt, Long life nickel electrodes for a nickel–hydrogen cell: results of an accelerated test and failure analyses, *Proc. 19th IECEC, August, 1984*, p. 312.

3 H. S. Lim and S. A. Verzwyvelt, Nickel electrodes expansion and the effect of LiOH additive, *Proc. 20th IECEC, August, 1985*, p. 1.104.

4 M. P. Bernhardt and D. W. Mauer, *Proc. 29th Power Sources Conf., 1980*, The Electrochemical Society, Pennington, NJ, p. 219.

5 P. P. McDermott, Analysis of nickel electrode behavior in an acccelerated test, in R. G. Gunther and S. Gross (eds.), *Proc. Symp. on the Nickel Electrode, Proc. Vol. 82-4*, The Electrochemical Society, Pennington, NJ, 1982, p. 224.

6 V. A. Tracy, *Powder Metall., 9* (1966) 54.